

# Lawrence Berkeley National Laboratory

## Recent Work

### Title

ALUMINA SCALE ADHERENCE TO CoCrAl ALLOYS AND COATINGS

### Permalink

<https://escholarship.org/uc/item/4zc7t95k>

### Authors

Whittle, D.P.

Boone, D.H.

### Publication Date

1981-04-01

c.2



# Lawrence Berkeley Laboratory

UNIVERSITY OF CALIFORNIA

RECEIVED  
LIBRARY  
BERKELEY, CALIFORNIA

## Materials & Molecular Research Division

JUN 2 1981

LIBRARY  
DOCUMENTS

Presented at the 7th LBL/MMRD International Materials Symposium, 17th University Conference on Ceramics, Surfaces and Interfaces in Ceramic and Ceramic-Metal Systems, Lawrence Berkeley Laboratory, University of California, Berkeley, CA, July 28-30, 1980

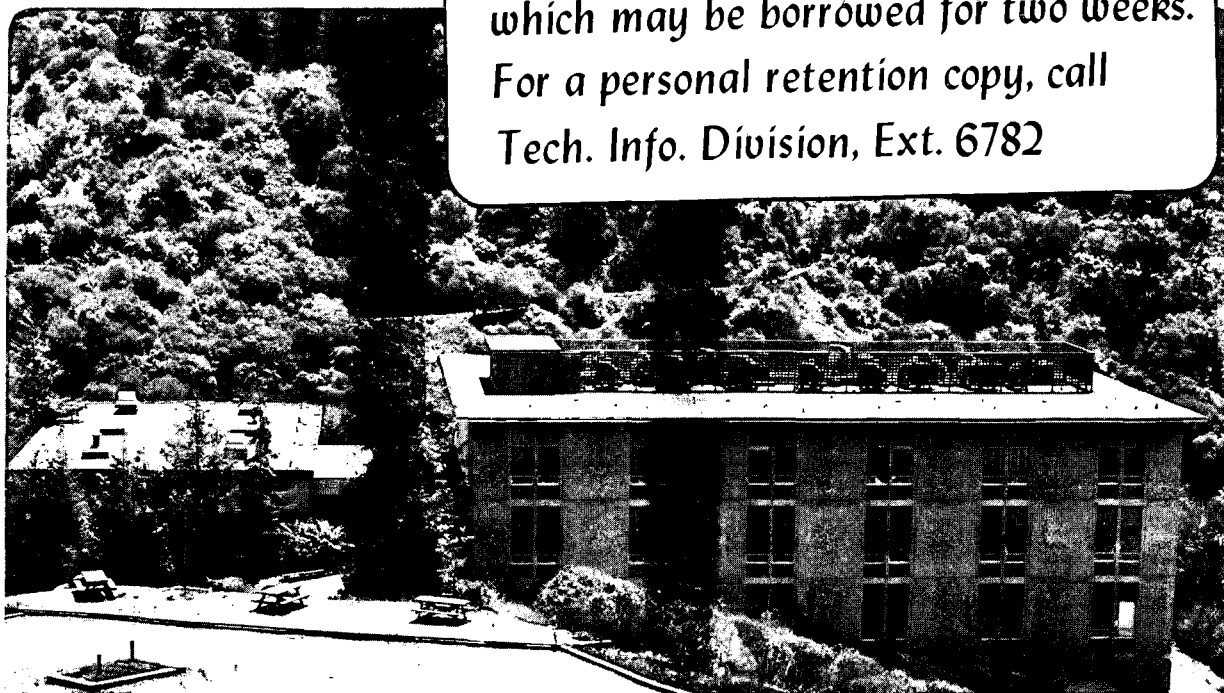
ALUMINA SCALE ADHERENCE TO CoCrAl ALLOYS AND COATINGS

D.P. Whittle and D.H. Boone

April 1981

**TWO-WEEK LOAN COPY**

*This is a Library Circulating Copy  
which may be borrowed for two weeks.  
For a personal retention copy, call  
Tech. Info. Division, Ext. 6782*



LBL-12421  
c.2

## **DISCLAIMER**

This document was prepared as an account of work sponsored by the United States Government. While this document is believed to contain correct information, neither the United States Government nor any agency thereof, nor the Regents of the University of California, nor any of their employees, makes any warranty, express or implied, or assumes any legal responsibility for the accuracy, completeness, or usefulness of any information, apparatus, product, or process disclosed, or represents that its use would not infringe privately owned rights. Reference herein to any specific commercial product, process, or service by its trade name, trademark, manufacturer, or otherwise, does not necessarily constitute or imply its endorsement, recommendation, or favoring by the United States Government or any agency thereof, or the Regents of the University of California. The views and opinions of authors expressed herein do not necessarily state or reflect those of the United States Government or any agency thereof or the Regents of the University of California.

## ALUMINA SCALE ADHERENCE TO CoCrAl ALLOYS AND COATINGS

D.P. Whittle and D.H. Boone

MMRD, Lawrence Berkeley Laboratory and  
Department of Materials Science and Mineral Engineering  
University of California  
Berkeley, California 94720

### INTRODUCTION

There are two essential requirements for alloys or coatings which are designed to withstand degradation by oxidation during high temperature exposure. First, they must form a surface oxide which thickens only at a slow rate, and secondly this oxide layer must remain adherent to the alloy surface under all conditions.  $\text{Al}_2\text{O}_3$  is generally regarded as the best protective oxide: diffusion through  $\text{Al}_2\text{O}_3$  is relatively slow in comparison with most other oxides, and since it is also stable, relatively little difficulty exists in selecting a composition which contains sufficient aluminium to provide, by selective oxidation, a protective  $\text{Al}_2\text{O}_3$  scale under various service environments. Typically, these will contain at least 5% Al (by mass) and usually substantial amounts of Cr.

Even though an alloy contains sufficient aluminium to develop the protective oxide, this usually does not occur immediately on exposure to an oxidizing atmosphere. When oxygen is admitted to a clean alloy surface at elevated temperatures, nuclei of all possible oxides are formed, and the amounts of these oxides are such that the proportion of metal atoms is essentially the same as that of the surface of the alloy. The different nuclei grow laterally, covering the surface at rates which cannot be predicted. In addition, they grow outwards and the base metal oxides tend to outgrow the protective oxide,  $\text{Cr}_2\text{O}_3$  or  $\text{Al}_2\text{O}_3$ . However, because of its greater stability, the protective oxide will continue to grow laterally, until eventually the alloy surface is covered with a continuous layer of this oxide. At this point, growth of the base metal oxides will to all intents and purposes cease, and thereafter the

overall oxidation rate is controlled by the growth of the protective oxide layer.

The second requirement is that of adhesion, the bonding of the ceramic oxide to the substrate, since during exposure environmental changes or stresses accompanying scale growth can cause loss of adhesion and spallation of the oxide. Numerous factors may affect oxide adhesion, but if consideration of mechanical disturbance is neglected, probably that of most importance is thermal cycling. During heating or cooling, stresses are developed owing to differences in thermal expansion or contraction of the oxide and alloy and these can lead to spallation of the protective oxide and excessive rates of metal loss.

Empirically, it was discovered over 40 years ago that additions of rare earth metals as a melt deoxidant to Nichrome (Ni-20%Cr) heating elements produced substantial increases in their lifetimes to failure in cyclic heating and cooling tests<sup>1</sup>: the protective oxide was more adherent. Subsequent work has confirmed that a wide range of additions can have a similar effect. Indeed, fine distributions of stable oxides in the alloy are perhaps even more effective in improving an alloy's performance under thermal cycling conditions. In many cases the two effects are indistinguishable, and may indeed be identical. Improvement in scale adhesion is not the only beneficial effect, although it is usually the most dramatic. The initial development of the protective oxide may also be modified with additions generally promoting the selective oxidation of chromium or aluminium from the alloy. The growth rate of the scale may also be reduced, although it is often difficult to distinguish from this the effects related to increased scale-alloy adhesion.

The most important group of alloys, other than the conventional heater alloys, to which active elements are added is the MCrAlY group of overlay cladding alloys where M is Fe, Ni or Co. These alloys are widely used for protecting gas turbine blades exposed to severe environments, and it appears that those with a cobalt base have significantly higher resistance. Alumina-forming coatings or claddings are degraded principally by the progressive loss of oxide as a result of thermal cycling; the principal role of yttrium is therefore to improve the adhesion. However, Y may not be the optimum active element for improving the overall oxidation resistance. In addition, it is clear that the structure of the alloy or coating, and in particular the distribution of the active element,<sup>5</sup> will depend on the processing technique. Studies by Gupta<sup>2</sup> indicate differences between EB-PVD (electron beam physical vapor deposition) and PS (plasma-sprayed) applied coatings of the same composition: as cast alloys might also be expected to behave differently.<sup>6</sup>

The present paper, therefore, examines the behavior of a number of CoCrAl alloys and coatings containing different active

element additions. All the compositions studies contain more than sufficient Al to ensure rapid, initial formation of a protective  $\text{Al}_2\text{O}_3$  scale and as a consequence, attention is focussed on the scale/substrate adhesion, rather than the development of the initial protective oxide.

#### EXPERIMENTAL OBSERVATIONS

Yttrium and hafnium additions to Co-10Cr-11Al alloys appeared to decrease the isothermal oxidation rate at  $1100^\circ\text{C}$ <sup>3,4</sup>, although Giggins & Pettit<sup>5</sup> maintained that Y additions to Co-25Cr-6Al had virtually no effect under isothermal conditions. These latter authors suggested the oxidation rate fitted a parabolic rate law. However, although undoped Co-10Cr-11Al followed an approximate parabolic law, the oxidation rate of the Hf- or Y-doped alloys decreased at a much faster rate than was consistent with diffusion-controlled growth.<sup>4</sup> Furthermore, increasing the Hf and Y content tended to reduce the duration of the initial transient oxidation stage and speed up the establishment of a continuous  $\text{Al}_2\text{O}_3$  layer. Figure 1 compares the mass gain after 100 h exposure at  $1100^\circ\text{C}$  for the various alloys. On the undoped alloys, the mass gain ranges from 0.53 to 0.82  $\text{mg}/\text{cm}^2$ : there is no real systematic variation with alloy composition, although the higher chromium content alloys are perhaps slightly better. For additions of Hf the maximum effect is with the smallest hafnium addition. Under thermal cycling conditions, the maximum effect was obtained at higher hafnium levels, 0.3-1.0%.

Metallographic evidence indicated differences between the doped and undoped alloys<sup>3-5</sup>: similar effects were found in  $\text{Al}_2\text{O}_3$ -forming iron-based alloys.<sup>6</sup> First, the alloy surface after the  $\text{Al}_2\text{O}_3$  scale had been removed was completely covered with imprints of the oxide grains for the doped alloys whereas there were numerous smooth areas, representing areas of no contact between scale and alloy, for the addition-free alloys. Examples of these are shown in Figure 2. A 0.05% addition was sufficient to eliminate these voids.

The second major difference was the presence of intrusions of oxide growing into the alloy from the surface scale. These intrusions were principally  $\text{Al}_2\text{O}_3$  that had apparently grown around particles of internally formed active element oxide. The morphology of the oxide intrusions was different for Y- and Hf-containing alloys, and alloys containing an  $\text{HfO}_2$  dispersion. These latter had been prepared by internal oxidation of Co-10Cr-11Al-Hf in a low oxygen activity pack such that only Hf, and not Cr or Al, were converted to oxide.<sup>7</sup> Figure 3 shows the underside of the  $\text{Al}_2\text{O}_3$  scales after dissolving away the underlying metal using a MeOH-10% Br solution.

Figure 4 compares the morphological features, as viewed in section of the  $\text{Al}_2\text{O}_3$  scales formed after 240h oxidation at  $1000^\circ\text{C}$

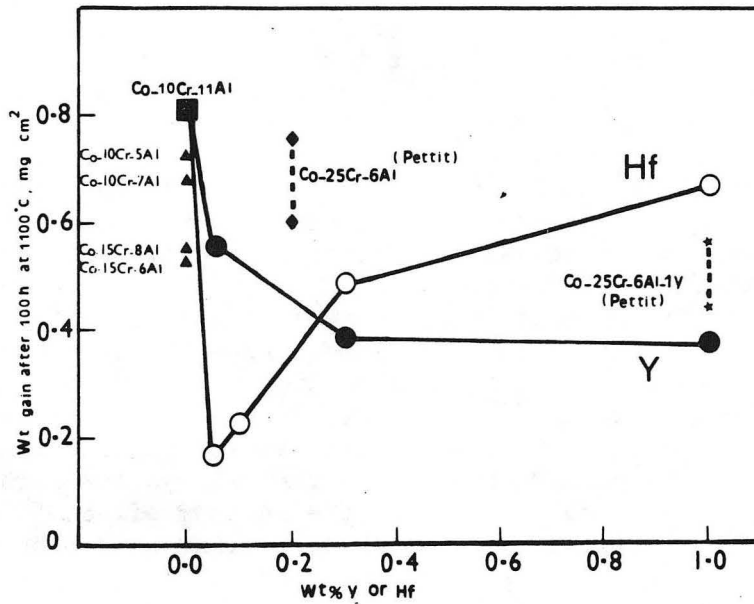


Fig. 1. The effect of Hf and Y in Co-10Cr-11Al on the mass gain after 100h exposure at 1100°C in air.<sup>4,5</sup>

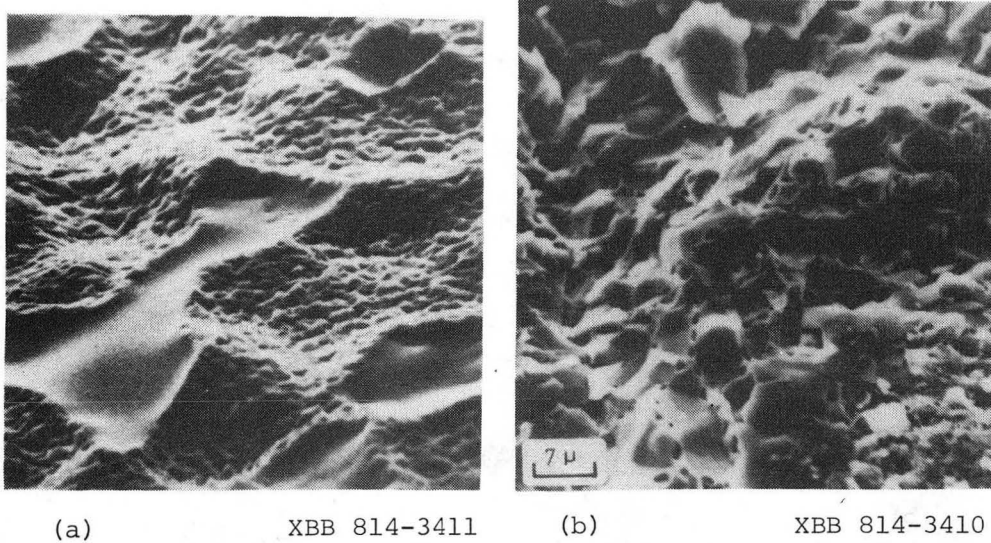
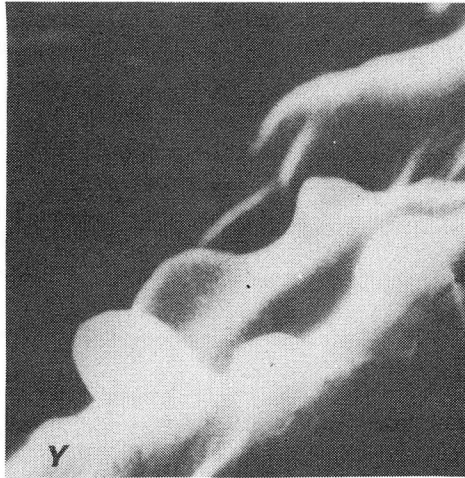
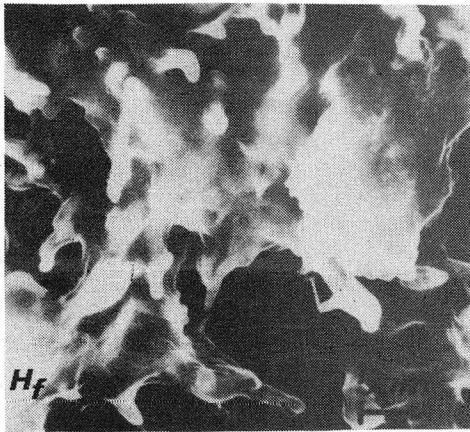


Fig. 2. The alloy surface after removal of the scale of a specimen of (a) Co-15Cr-8Al oxidized for 190h at 1200°C (micron mark = 20  $\mu\text{m}$ ) and (b) Co-10Cr-11Al-0.1Y oxidized for 1000h at 1200°C (micron mark = 10  $\mu\text{m}$ ). The surface of the Y-containing alloy is completely imprinted with oxide grains; that of the Y-free alloy contains smooth, imprint-free regions where the scale was not in contact with the alloy.

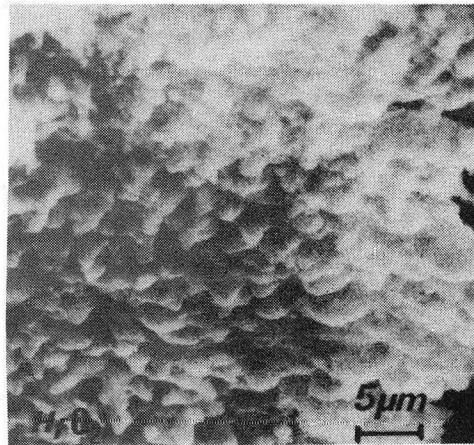




(a)



(b)



(c)

Fig. 3. A comparison of the underside of the  $\text{Al}_2\text{O}_3$  scale, stripped from the alloy. (a) Co-10Cr-11Al-0.3Y oxidized for 75h at  $1200^\circ\text{C}$ . (b) Co-10Cr-11Al-Hf oxidized for 75h at  $1200^\circ\text{C}$ . (c) Co-10Cr-11Al-1Hf, internally oxidized in a CoAl- $\text{Al}_2\text{O}_3$  mixture for 200h at  $1200^\circ\text{C}$  to convert the Hf into an oxide dispersion, and then oxidized for 75h at  $1200^\circ\text{C}$  (micron mark =  $5\ \mu\text{m}$ ). XBB 814-3409

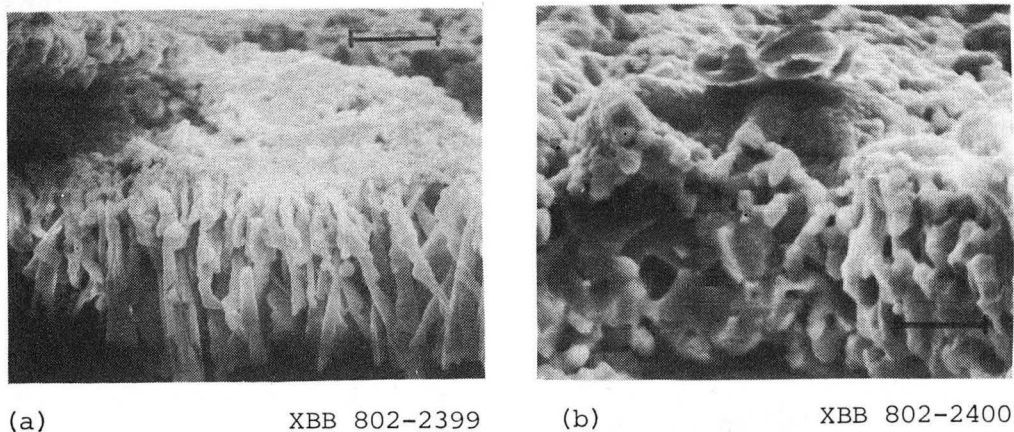


Fig. 4. SEM sections of the oxides stripped from (a) CoCrAlHf, (b) CoCrAlSi after oxidation for 240h in air at 1000°C. (micron mark = 10 $\mu$ ).

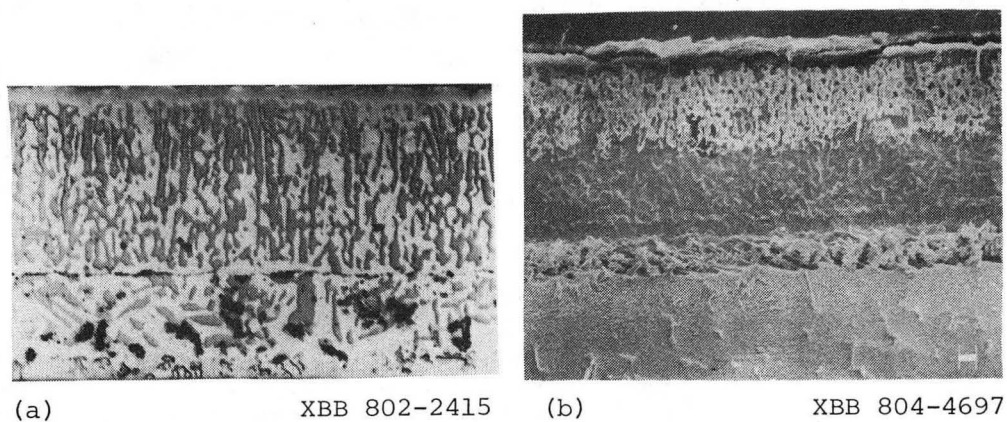


Fig. 5. Cross-section of the CoCrAl coating after oxidation for 240h at 1000°C. (a) Metallographic section and (b) after deep etching. (micron mark = 20  $\mu$ m).

on EB-PVD Co-20Cr-10Al coatings containing different active element additions. The coatings were prepared by Airco Temescal under DOE contract no. ET-78-C-03-2156. This latter program was a study<sup>8</sup> of the ability to deposit multi-element coatings with low vapor pressure additions; some samples represent addition levels higher than might be used in actual practice. The coatings were all 100-125  $\mu\text{m}$  thick and deposited on IN 738 substrates.

The oxide grain structures fall into two broad categories. A columnar-type structure with the grains orientated in the growth direction and single grains penetrating almost completely through the scale section. This is typified in Figure 4a by the oxide formed on the Hf containing coating; the oxide on the Y-containing coating is very similar. The second type of oxide has an equiaxed, granular-type of structure. Figure 4b shows the scale on the coating with no addition: those formed on the coatings containing Zr, Si, Ti are similar. The grain size of the oxide parallel to the growth direction is very similar in both columnar and granular scales.

Comparison of the undersides of the  $\text{Al}_2\text{O}_3$  scales after the substrate had been dissolved away, again showed two types of morphology. With the Hf-containing coating the underside of the oxide had an irregular appearance with numerous fingers of oxide penetrating out of the scale into the substrate. These are the oxide pegs referred to earlier. They are more angular in nature than those observed with cast CoCrAlHf alloys,<sup>4</sup> and also more abundant. However, this latter factor may well be related to the higher Hf content, 1.5% compared to the 0.3-1.0% in the cast alloys. In spite of this, Hf could not be detected by EDAX analysis of the undersides of the oxide.

The second-type of scale underside, typical of the granular  $\text{Al}_2\text{O}_3$  scales formed on the Si- and Zr-containing coatings showed less pronounced protrusions. In relation to the earlier work,<sup>4</sup> this type of morphology would not give as an adherent scale as the more angular pegs developed in the Hf-containing compositions. The underside of the oxides on the Ti-containing coating and the addition-free coating also had a plate-like morphology, and in fact EDAX analysis of the feathery plates indicates significant concentration of Ti. Both the Y- and Si-containing coatings also show significant Ti concentrations, and oxide platelet formation at the scale/coating interface. The Ti has presumably diffused out through the coating from the IN 738 substrate. Again these poorly distributed pegs and platelets are unlikely to produce the maximum scale/substrate adherence.

A typical metallographic section through the coating after the 240h exposure at 1000°C is shown in figure 5a. This particular micrograph is of the CoCrAl coating containing no addition elements.

The coating consists of a dark, dendritic  $\beta$ -CoAl phase in a lighter  $\alpha$ -Co-rich matrix. The  $\beta$ -phase is orientated normal to the growth direction of the coating. In addition, there is also a band at the surface of the coating, which is devoid of the  $\beta$ -phase. This is formed as a result of the loss of Al from the surface to form the  $\text{Al}_2\text{O}_3$  scale during oxidation. The  $\text{Al}_2\text{O}_3$  scale is not visible in the optical micrograph, because of its poor contrast with the other phases. It can, however, be revealed by adjusting the lighting conditions.

An additional feature of the coating is that the  $\beta$ -phase in the outer half of the coating is a slightly darker color than that in the inner half of the coating. The reason for this only became apparent when the sample was deep etched in MeOH-10%Br solution, sufficient metal being removed so that the underside of the oxide could be examined. This technique has considerable advantage over the complete stripping of the oxide, in that the detailed oxide morphology can be related to the coating structure. Figure 5b shows the resulting microstructure. The  $\beta$ -phase in the outer half of the coating is sheathed with  $\text{Al}_2\text{O}_3$ . Presumably this sheath is very thin, since there is no indication of its presence in the optical micrograph. The surface  $\text{Al}_2\text{O}_3$  scale is also visible in Figure 5b and it is clear that this is not attached to the  $\text{Al}_2\text{O}_3$  sheaths or pegs penetrating into the alloy. The  $\text{Al}_2\text{O}_3$  pegs do not cross the  $\beta$ -depleted zone. These observations throw quite a different light on the mechanism of peg formation: it appears to be related to preferential diffusion of oxygen inwards along the  $\alpha/\beta$  interface, and not to the presence of oxide particles in the alloy. The Si-containing coating behaves in a similar way.

Nevertheless, differences between the coatings containing different active elements are apparent. Figure 6 shows the deep etched structures of the oxides formed on the CoCrAlY and CoCrAlHf coatings. In the former case, peg growth again appears to have proceeded down the  $\alpha/\beta$  phase boundaries, although there is an important difference between this and the CoCrAl coating shown in Figure 5, in that the pegs or  $\text{Al}_2\text{O}_3$  sheaths are now attached to the surface scale. With the Hf-containing coating, Figure 6b, a profuse distribution of pegs is attached to the surface scale, and these do not seem to penetrate down the  $\alpha/\beta$  boundaries of the coating. Indeed, there is a  $\beta$ -free region immediately below the pegged scale. These inwardly growing pegs presumably grew around internal oxide particles of  $\text{HfO}_2$ , as observed with the as-cast alloys.

In an attempt to obtain a semi-quantitative measure of the scale adhesion, a simple, room temperature erosion test was carried out. This consisted of eroding oxidized samples of the coatings with SiC particles at a  $30^\circ$  angle of incidence. The mass of incident SiC erodent to produce exposed metal may be taken as a tentative measure of the scale adhesion and this is tabulated in

Table I. However, it must be remembered that the thickness of the  $\text{Al}_2\text{O}_3$  was different on the different coatings. Nevertheless, the  $\text{Al}_2\text{O}_3$  scale appears to be more adherent on the Hf-containing coating, with the Y-containing being next: an order consistent with the observed morphological features.

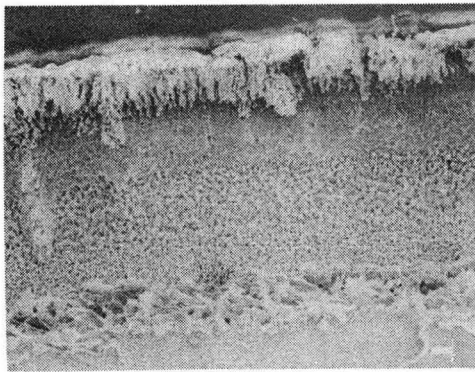
#### MECHANISM OF IMPROVED SCALE ADHESION

A number of hypotheses have been put forward to account for the improved scale adhesion, and these and other aspects of the "active element effect" have been reviewed in detail.<sup>9</sup> Essentially most of the theories are independent of whether the alloy contains a metallic addition of the active element or a dispersion of its stable oxide. As pointed out earlier, because of the high affinity for oxygen of the active elements, they will be oxidized preferentially to chromium or aluminium, and as the addition is only present at a low concentration, the resulting oxides are in the form of discontinuous internal oxide particles in the alloy substrate ahead of the oxide-alloy interface. The distribution of the oxides may be very different in the two cases: those formed during high temperature oxidation are often formed in the vicinity of alloy grain boundaries at intersections with the scale-alloy interface. In dispersion-containing alloys, the distribution is generally more random. With coatings, the distribution of any internal oxides may well be more related to the coating structure, or indeed the active element could be oxidized during the coating process itself.

The most important mechanistic models explaining the improved scale adherence, although it must be realized that these are not necessarily mutually exclusive, are: (a) enhanced scale plasticity; (b) graded seal mechanism; (c) modification to growth process; (d) chemical bonding; (e) vacancy sink model; (f) oxide pegging.

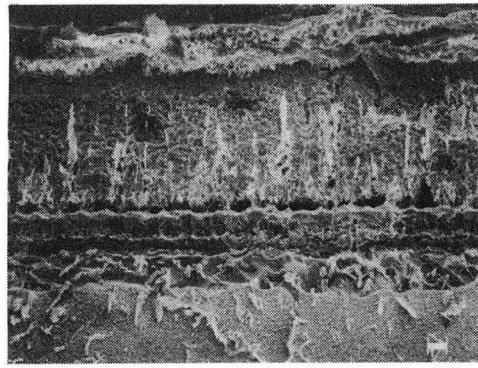
Table I. Adherence of  $\text{Al}_2\text{O}_3$  as Determined by  
Resistance to SiC Erosion

Coating	CoCrAlHf	CoCrAlY	CoCrAlTi	CoCrAlSi	CoCrAl	CoCrAlZr
Surface Oxide thickness $\mu\text{m}$	2	3	4	10	8	14
SiC mass to expose bare metal, g	11	9	5.2	5.2	4.5	3.2



(a)

XBB 804-4705



(b)

XBB 804-4703

Fig. 6. Deep etched structures of the oxides formed on (a) CoCrAlY (micron mark = 10  $\mu\text{m}$ ) and (b) CoCrAlHf after oxidation for 240h at 1000°C. (micron mark = 5  $\mu\text{m}$ ).

(a) Enhanced Scale Plasticity

It has been proposed<sup>6,10,11</sup> that elements such as yttrium may improve the adhesion of  $\text{Al}_2\text{O}_3$  on alloys by causing the  $\text{Al}_2\text{O}_3$  to be more easily deformed and thereby allowing the relief of growth and thermally induced stresses that would otherwise have caused spallation of the  $\text{Al}_2\text{O}_3$ . Grain boundary sliding is expected to be the major deformation mechanism in the scale, and it has been suggested that a fine-grained oxide can more easily accommodate growth and thermally induced stresses by grain boundary sliding than larger grained oxide.<sup>6</sup> Kuenzly and Douglass,<sup>12</sup> however, have suggested that the oxide scale plasticity is actually decreased by the addition of yttrium since  $\text{Y}_2\text{O}_3$ ,  $\text{YAlO}_3$  and  $\text{Y}_3\text{Al}_5\text{O}_{12}$  (YAG-garnet) form at grain boundaries and inhibit plastic deformation of  $\alpha\text{-Al}_2\text{O}_3$  by a grain boundary sliding mechanism.

Hollenberg & Gordon<sup>12</sup> studied the effects of different dopants on the creep behaviour of polycrystalline  $\text{Al}_2\text{O}_3$  and found that doping with either  $\text{Fe}^{2+}$  or  $\text{Ti}^{4+}$  resulted in the creation of either Al-ion interstitials or Al-ion vacancies respectively. Both species enhanced the cation diffusion rate and increased the creep rate. The creep rate of  $\text{Cr}^{3+}$ -doped  $\text{Al}_2\text{O}_3$  was comparable to that of undoped  $\text{Al}_2\text{O}_3$  of similar grain size. Thus, there is no conclusive evidence that the deformability of  $\text{Al}_2\text{O}_3$  is modified by the incorporation of either active elements, or oxide particles within the scale and it is unlikely that an oxide plasticity model is of particular significance: often there is more apparent deformation of the  $\text{Al}_2\text{O}_3$  scale on undoped or dispersion-free alloys in any case.

Deformation of the alloy is possibly another means whereby stress relief can occur. Golightly et al.<sup>14</sup> observed apparent deformation of the alloy when a ridged alloy surface developed during  $\text{Al}_2\text{O}_3$  growth. However, the loads required to deform typical  $\text{Al}_2\text{O}_3$ -forming alloys were not particularly affected by yttrium concentration.<sup>5</sup>

(b) Graded Seal Mechanism

The graded seal mechanism is based on the supposition that a layer of compound oxide is developed between the surface scale and the alloy, which has a thermal expansion coefficient intermediate between that of the scale and the substrate.<sup>15</sup> However, as indicated in Section 2, there are very few systems in which a complete or even partial layer of a compound oxide has been observed.

(c) Modification to Growth Process

$\text{Al}_2\text{O}_3$  grows primarily by oxygen transport, albeit via short circuit paths.<sup>6,11</sup> Generally, higher levels of growth stress would be expected to be associated with anion-conducting scales<sup>16</sup> since

the new oxide is formed under constraint at the alloy-scale interface.

Golightly et al.<sup>14</sup> have suggested that in addition to inward oxygen diffusion down the  $\text{Al}_2\text{O}_3$  grain boundaries, outward diffusion of aluminium occurs, probably along line defects in the oxide. Reaction between the inward- and outward-diffusing species results in the formation of oxide within the existing scale layer. Hence, lateral growth of the oxide occurs as oxidation proceeds, leading to the rapid development of high compressive stresses and consequent localized detachment of the scale from the underlying alloy. They suggest that the continuing lateral growth of the scale results in the development of a 'convoluted morphology' of the oxide leading to oxide detachment at temperature and extensive spallation during cooling. Based on this model, the increased adherence of the scale due to Y-additions was mainly attributed to the prevention of the formation of convoluted morphologies: incorporation of yttrium into the scale suppresses the cation contribution to scale growth and therefore reduces oxide formation within the existing oxide layer.

The three mechanisms outlined so far are all based on the concept that the effect of the addition produces less stress in the scale-alloy system, or that the system is able to accommodate that stress more effectively. However, Giggins & Pettit<sup>5</sup> performed the following simple experiment: oxidized samples of CoCrAlY and CoCrAl were bent at room temperature. Scale spallation was far more pronounced from the CoCrAl samples and thus a major effect of the addition is to improve adhesion and any model which proposes improved adhesion because of stress relief or the absence of stress development cannot be wholly acceptable.

(d) Chemical bonding

The adhesion of the scale to the substrate is clearly dependent on the nature of the atomic bonds which are developed across the oxide-alloy interface. McDonald & Eberhart<sup>17</sup> found that impurities that are highly oxygen-active can make a major contribution to the adhesive force at the interface. However, arguing against this being a major factor is the fact that  $\text{Al}_2\text{O}_3$  dispersions in  $\text{Cr}_2\text{O}_3$ -forming alloys do produce identical improvements in scale adherence:  $\text{Al}_2\text{O}_3$ - $\text{Cr}_2\text{O}_3$  solid solutions show little deviation from thermodynamically ideal behaviour. An even more convincing argument is that the presence of an  $\text{Al}_2\text{O}_3$  dispersion in Fe-25Cr-41Al, an  $\text{Al}_2\text{O}_3$ -forming alloy, also results in a significant increase in adhesion, which obviously cannot be explained in terms of a chemical bonding mechanism.<sup>6</sup>



(e) Vacancy Sink Model

There has been clear evidence that the presence of an active metal (Figure 2 and ref. 6) or an oxide dispersion in the alloy minimizes the development of voids at the alloy-scale interface. It has been proposed<sup>6,16</sup> that the internal oxide particles of the active element, the active element atoms themselves or the stable oxide dispersion provide alternative sites for vacancy condensation, thus eliminating interfacial porosity. This, in turn, helps to maintain scale-metal contact and minimize scale spallation. There are some questions, however, as to the source of the vacancies.<sup>8</sup> Kuenzly & Douglass<sup>12</sup> have suggested that it might arise from a Kirkendall effect in the alloy substrate, associated with the selective removal of one of the alloy components, and the unequal flux of the more noble components away from the alloy-scale interface. In view of the very slow rates of scale growth, however, particularly with  $\text{Al}_2\text{O}_3$ , such a vacancy flux would be quite small.

(f) Oxide Pegging

Mechanical keying of the oxide to the alloy substrate, as a result of the internal oxidation of the active alloying addition, or dispersoid particles growing in size to form 'oxide stringers' of thin elongated oxide intrusions extending into the alloy substrate, has been suggested by many authors (see ref. 9). Earlier models suggested that the oxide peg consisted of the active element oxide itself, or a compound oxide between it and the main scale-forming constituent. However, the present work has shown that the pegs consist primarily of  $\text{Al}_2\text{O}_3$ . Originally<sup>4,7</sup> it was postulated that these form by enhanced inward growth of that oxide along the incoherent boundary between the active element oxide and the metallic substrate. This is still the case. However, in addition, the incoherent  $\alpha/\beta$  phase boundaries also appear capable of acting as easy paths for the inward growth of the oxide. The number of pegs which develop seems to be important. An addition of 0.05% Hf or Y to Co-10Cr-11Al is sufficient to minimize scale spallation and improve overall oxidation resistance under isothermal conditions, but not under thermal cycling conditions. Additions of 0.3 and 1.0% Hf appear to be optimum.

In cast alloys hafnium additions seem more efficient than yttrium, and this is related to the shape of the pegs as much as to concentration. With the hafnium additions, the internal growth of  $\text{Al}_2\text{O}_3$  around the Hf-rich internal oxide particles takes on a branched, dendritic form as opposed to the relatively smooth interface between the  $\text{Al}_2\text{O}_3$  surrounding the Y-rich particles and the alloy. These differences may well be related to the distribution of the active element in the original alloy. Yttrium tends to segregate to grain boundaries as an intermetallic yttride; hafnium is completely in solid solution, and thus leads to a very fine

distribution of small, internal oxide precipitates which then promote the branching growth of  $\text{Al}_2\text{O}_3$  around them. There is also some evidence to suggest that enrichment of yttrium may occur in the internal oxide zone, promoting growth of larger particles. This may also explain why peg growth in the CoCrAlY coating is apparently able to bridge the  $\beta$ -depleted zone and peg development continue down the  $\alpha/\beta$  phase boundaries. This again leads to excessive peg development which can be detrimental.

Peg development in the addition-free, Ti, Si and Zr-containing coatings is primarily down  $\alpha/\beta$  phase boundaries, and as such they do not cross the  $\beta$ -free zone and thus do little to improve adhesion. Neither Ti, Si nor Zr are active elements in  $\text{Al}_2\text{O}_3$ -forming alloys, in the sense that their oxides are less stable than  $\text{Al}_2\text{O}_3$ . They, therefore, will not develop pegs attached to the surface scale unless  $\beta$ -phase is present at that interface.

#### CONCLUDING REMARKS

The formation of oxide pegs, though not the only factor, is perhaps the most decisive in improving the oxide adhesion. The pegs appear to form by preferential oxygen diffusion into the alloy or coating surface along incoherent interfaces. These interfaces may be either between the  $\alpha$  and  $\beta$  phases in the metallic structure, or between an oxide dispersion and the matrix, the oxide dispersion being added intentionally during the processing, or as a result of internal oxidation of an active element addition during high temperature exposure. Pegs developed around active element oxides are generally better, since these are usually attached to the surface scale. Furthermore, the distribution of the oxide dispersion, and subsequently the pegs, can be better controlled if this is produced prior to exposure.

#### ACKNOWLEDGEMENTS

This work has been supported by the Division of Materials Science, Office of Basic Energy Sciences, U.S. Department of Energy under Contract No. W-7405-ENG-48. The coated samples were prepared under DOE Contract No. Et-78-C-03-2156. We are also grateful to Mr. S. Shaffer and Mr. J. Maasberg for the metallographic examinations and erosion studies respectively.

## REFERENCES

1. L.B. Pfeil, U.K. Patent no. 459848 (1937); no. 574088 (1945).
2. D. Gupta, Thin Solid Films 63, 542 (1979).
3. J. Stringer, I.M. Allam & D.P. Whittle, Thin Solid Films 45, 377-384 (1977).
4. I.M. Allam, D.P. Whittle, & J. Stringer, Oxidat. Metals 12, 35-67 (1978).
5. C.S. Giggins & F.S. Pettit, Wright Patterson Air Force Base, Contr. no. F33615-72-C-1072 (1975).
6. J.K. Tien & F.S. Pettit, Metall. Trans 3, 1587-1599 (1972).
7. I.A. Allam, D.P. Whittle & J. Stringer, Oxidat. Metals 13, 381-402 (1978).
8. D.H. Boone, S. Shen & R. McKoon, Thin Solid Films 63, 299 (1979).
9. D.P. Whittle & J. Stringer, Phil. Trans. Roy. Soc., London A295, 309 (1980).
10. J.E. Antill, & K.A. Peakall, J. Iron Steel Inst. 205, 1136-1142 (1967).
11. J.M. Francis & J.A. Jutson, Corros. Sci. 8, 445-449 (1968).
12. J.D. Kuenzly & D.L. Douglass, Oxidat. Metals 8, 139-178 (1974).
13. G.W. Hollenberg & R.S. Gordon, J. Am. Ceram. Soc. 56, 140-144 (1972).
14. F.A. Golightly, F.H. Stott & G.C. Wood, Oxidat. Metals 10, 163-187 (1976).
15. H. Pfeiffer, Werkst. Korros, Mannheim 8, 574 (1957).
16. J. Stringer Corros. Sci. 10, 513-543 (1970).
17. J.E. McDonald & J.G. Eberhart, Trans. Metall Soc. A.I.M.E. 233, 512-517 (1965).
18. E.J. Felten, J. Electrochem. Soc. 108, 490-495 (1971).

This report was done with support from the Department of Energy. Any conclusions or opinions expressed in this report represent solely those of the author(s) and not necessarily those of The Regents of the University of California, the Lawrence Berkeley Laboratory or the Department of Energy.

Reference to a company or product name does not imply approval or recommendation of the product by the University of California or the U.S. Department of Energy to the exclusion of others that may be suitable.

TECHNICAL INFORMATION DEPARTMENT  
LAWRENCE BERKELEY LABORATORY  
UNIVERSITY OF CALIFORNIA  
BERKELEY, CALIFORNIA 94720